
Content-Rich AIGC Video Quality Assessment via Intricate Text Alignment and Motion-Aware Consistency

Shangkun Sun^{*1,2} Xiaoyu Liang^{*1} Bowen Qu¹ Wei Gao^{1,2}

Abstract

The advent of next-generation video generation models like *Sora* poses challenges for AI-generated content (AIGC) video quality assessment (VQA). These models substantially mitigate flickering artifacts prevalent in prior models, enable longer and complex text prompts and generate longer videos with intricate, diverse motion patterns. Conventional VQA methods designed for simple text and basic motion patterns struggle to evaluate these content-rich videos. To this end, we propose **CRAVE** (**C**ontent-**R**ich **A**I**G**C **V**ideo **E**valuator), specifically for the evaluation of Sora-era AIGC videos. CRAVE proposes the multi-granularity text-temporal fusion that aligns long-form complex textual semantics with video dynamics. Additionally, CRAVE leverages the hybrid motion-fidelity modeling to assess temporal artifacts. Furthermore, given the straightforward prompts and content in current AIGC VQA datasets, we introduce **CRAVE-DB**, a benchmark featuring content-rich videos from next-generation models paired with elaborate prompts. Extensive experiments have shown that the proposed CRAVE achieves excellent results on multiple AIGC VQA benchmarks, demonstrating a high degree of alignment with human perception. All data and code will be publicly available.

1. Introduction

Recently, text-driven video generation (Brooks et al., 2024; Hunyuan, 2024) has seen significant growth. However, evaluating these text-driven AI-generated videos presents unique and escalating challenges. These challenges primarily stem from two key issues: (1) the need for precise video-text alignment, especially with complex and lengthy

text prompts; (2) the occurrence of distinct distortions that are not typically found in naturally generated videos, such as irregular motion patterns and objects.

With the advancement of new-generation video models, these challenges have become even more pronounced. These new-generation models, marked by the advent of *Sora* (Brooks et al., 2024), offer substantial improvement in generation quality compared to previous models, characterized by rich details and content, such as *Kling* (Kuaishou, 2024), *Gen-3-alpha* (Runway, 2024), *Vidu* (Shengshu, 2024), etc. Compared with previous AIGC videos, these models support **much longer and more intricate text prompt (often over 200 characters), as well as more complex motion patterns with longer duration (often over 5 seconds with the fps of 24)**. As illustrated in Figure 1, these rich contents impose greater demands on the evaluator’s ability to understand video dynamics and its relationship with complex textual semantics.

To address this, we introduce Content-Rich AIGC Video Evaluator (CRAVE), to assess the quality of these next-generation text-driven videos. CRAVE evaluates videos from three perspectives: It firstly considers the traditional visual harmony like the previous Video Quality Assessment (VQA) method (Wu et al., 2023a), which measures the aesthetics and distortions. Furthermore, CRAVE leverages a multi-granularity text-temporal fusion module to align the intricate texts with video dynamics. Additionally, CRAVE incorporates the hybrid motion-fidelity modeling that exploits hierarchical motion information to assess the temporal quality of the next-generation AIGC videos.

Besides, the gap between the naturalness and complexity of the latest AIGC videos and previous videos has become markedly apparent. To better assess current AIGC videos, we introduce CRAVE-DB, a content-rich AIGC VQA benchmark consisting of 1,228 elaborate text-driven videos generated by advanced models such as *Kling* (Kuaishou, 2024), *Qingying* (Zhipu, 2024), *Vidu* (Shengshu, 2024), and *Sora* (Brooks et al., 2024). Here, by “elaborate text,” we mean prompts that include complete descriptions of the subject, actions, and environment, with at least **5** detailed descriptions for any one aspect and a total character count exceeding **200**. These videos have largely eliminated is-

^{*}Equal contribution ¹SECE, Peking University
²PengCheng Laboratory. Correspondence to: Wei Gao
 <gaowei262@pku.edu.cn>.



Figure 1. Comparison of concurrent and previous AIGC videos. Videos are generated by Lavie (Wang et al., 2023c) (1st row) and Sora (Brooks et al., 2024) (2nd row), respectively. Nouns that should be present in the video are highlighted in orange, while adjectives with more details are highlighted in blue. The new-generation AIGC videos contain richer content.

sues prevalent in previous generations, such as flickering, weak motion, and short content. They encompass diverse scenes, subjects, actions, and rich details, with a duration of over 5 seconds and a frame rate of 24 fps. Extensive experiments show that CRAVE has achieved leading human-aligned video quality assessment results across multiple metrics on T2V-DB (Kou et al., 2024b), currently the largest AIGC VQA dataset, and the proposed CRAVE-DB.

To summarize, our main contributions are as follows: (1) We introduce CRAVE, the effective evaluator for content-rich videos derived from the new-generation video models, which assess AIGC videos from the temporal and video-text consistency via effective motion-aware video dynamics understanding and multi-granularity text-temporal fusion module. (2) Given the gap between new-generation AIGC videos and previous ones, we introduce CRAVE-DB, a benchmark containing AIGC VQA samples produced by advanced models like Kling, etc., to facilitate the evaluation of contemporary content-rich AIGC videos. (3) Extensive experiments demonstrate the proposed CRAVE achieves excellent results on multiple AIGC VQA benchmarks with varying sources of videos and prompt lengths, showcasing a strong understanding of the quality of AIGC videos.

2. Related Work

2.1. Measurement for Text-to-Video Models

Currently, common methods used in evaluating text-driven generated videos include some objective metrics (Radford et al., 2021; Unterthiner et al., 2018; Salimans et al., 2016) and human-aligned methods (Kirstain et al., 2023; Qu et al., 2024; Kou et al., 2024b). Objective metrics such as CLIP-score (Radford et al., 2021) measure the mean cosine similarity between the text and each frame. IS (Salimans et al., 2016) utilizes the inception feature to measure the overall quality of image and video frames. Flow score (Huang et al., 2024b) calculates dynamic degree via optical flow

models such as (Teed & Deng, 2020; Sun et al., 2022a). However, these objective metrics do not align with human subjective perception and often evaluate videos from a single dimension. Some methods for evaluating natural video quality provide human-aligned overall evaluations (Wu et al., 2023a; 2022; Kou et al., 2023). DOVER (Wu et al., 2023a) assesses quality in terms of aesthetics and technicality. FastVQA (Wu et al., 2022) utilizes grid mini-patch sampling to assess videos efficiently while maintaining accuracy. Q-Align (Wu et al., 2023b) transforms the video quality assessment task into the generation of discrete quality level words via the Multimodal Large Language Model. StableVQA (Chai et al., 2023) measures video stability by separately obtaining the raw optical flow, semantic, and blur features. These methods are suitable for natural video quality assessment but do not consider the text-video alignment, which is key to the evaluation of text-driven videos. To address this, EvalCrafter (Liu et al., 2024b) assesses quality through a series of indicators including CLIP score, SD score, and natural video quality assessment methods. T2VQA (Kou et al., 2024b) incorporates a transformer-based encoder and Large Language Model to assess text-driven AIGC videos. TriVQA (Qu et al., 2024) explores the video-text consistency through cross-attention pooling and the recaption of Video-LLaVA. However, there are still relatively fewer VQA methods specifically for AIGC videos. With the growth of new-generation videos, the requirements for understanding video dynamics and text consistency are becoming increasingly demanding, posing greater challenges.

2.2. Text-to-Video Generation Method

With the surge of diffusion models (Rombach et al., 2022; Ho et al., 2020), a lot of video generation models emerge (Singer et al., 2023; Wang et al., 2023b;a; Blattmann et al., 2023; Chen et al., 2023a; Zheng et al., 2024; Lab & etc., 2024). They represent a significant breakthrough in video generation. However, videos produced by previous methods still tend to suffer from issues such

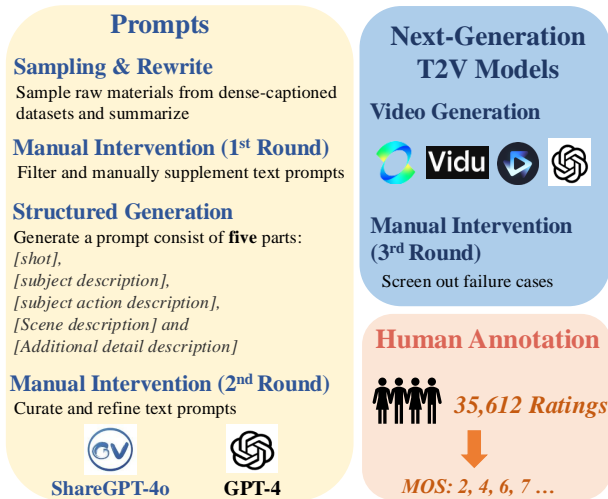


Figure 3. The collection of the proposed CRAVE-DB.

evaluating more sophisticated semantic alignment.

To address this, we propose to construct prompts with richer information. Our overall pipeline is shown in Figure 3. To ensure the prompts are detailed and semantically rich, we focus on the prior dense-captioned dataset, ShareGPT-4o dataset (Chen et al., 2023b), which leverages the advanced multimodal capabilities of GPT-4o to describe videos in detail. This dataset contains rich annotations that even require summarization to be clear prompts. We randomly sampled 300 captions from this dataset and summarized them using GPT-4 (Achiam et al., 2023), retaining only the key details. We then conducted the 1st round of manual intervention to filter out failed, redundant, or illogical generations.

Given that ShareGPT-4o primarily focuses on daily life scenarios, we manually crafted 200 more prompts to broaden the coverage of actions, subjects, and scenes. Prompts contain 4 categories: landscape, object, animal, and human. The “landscape” contains common scenes (e.g., grasslands, streets), rare environments (e.g., volcanoes, auroras), and renowned landmarks. The “animal” includes various mammals, reptiles, birds, fish, and amphibians. The “object” covers common real-world items, while the “human” features people across ages, genders, occupations, and clothing.

Subsequently, we employed GPT-4 to structure raw prompts using a template format: “[shot language] + [subject description] + [subject action description] + [scene description] + [additional detail description]”. The “shot language” incorporates various cinematographic techniques including tilt shots, flat shots, progressive shots, surround shots, close-ups, and panoramic views. The scene descriptions encompass natural landscapes under diverse weather and lighting conditions. Following this, we initiated a second round of manual intervention to screen and refine all prompts, ultimately finalizing a curated set of 410 high-quality prompts. The

overall word cloud is shown in Figure 2.

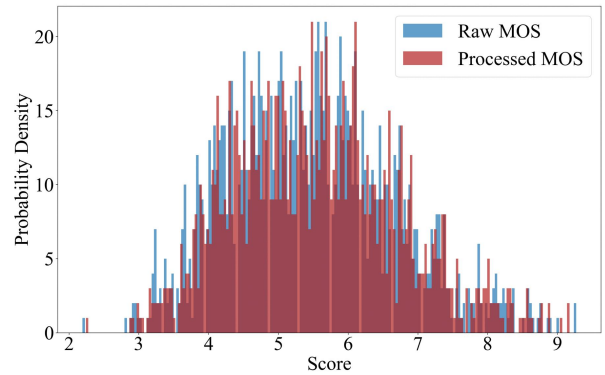


Figure 4. Distribution of MOS in CRAVE-DB.

3.2. Video Generation

Since the advent of Sora (Brooks et al., 2024), text-driven video generation methods have achieved significant advancements in visual quality, text understanding, and the diversity and complexity of generated content. Given the substantial gap between current AIGC videos and prior ones, constructing datasets using the next-generation video models is essential. In this work, we employ Sora and other subsequent state-of-the-art models: Kling (Kuaishou, 2024), Vidu (Shengshu, 2024), Qingying (Zhipu, 2024) to build samples. As Sora had not been publicly released by the time of our subjective evaluation, we curated 14 content-rich prompts and their corresponding outputs from Sora’s publicly showcased videos, resulting in a total of 1,228 videos. All videos exceed 5 seconds in duration with a frame rate of 24 fps, and resolutions ranging from 384×688 to 960×1440 , depending on the generation model. To evaluate newer video generation models and validate CRAVE’s 0-shot generalization capability, we utilized prompts from VideoGenEval (Zeng et al., 2024) to generate videos using recently accessible models such as Hunyuan (Hunyuan, 2024), Sora (post-API release), Seaweed Pro (ByteDance, 2024), Mochi 1 (Team, 2024) etc. These outputs were then evaluated using CRAVE, as shown in Figure 7. Compared with other datasets, VideoGenEval exhibits relatively higher prompt density (Table 1) and employs distinct prompts compared to CRAVE-DB. Despite its lack of annotations, it is suitable for 0-shot testing.

3.3. Subjective Study

According to ITU (Series, 2012) standards, subjective experiments should involve at least 15 participants to reduce error fluctuations. To obtain the Mean Opinion Score (MOS) for each video, in our experiment, each video was scored by 29 different human subjects. These participants come from diverse backgrounds, including science, engineering, business, law, etc., with all being over 18 years old. Prior

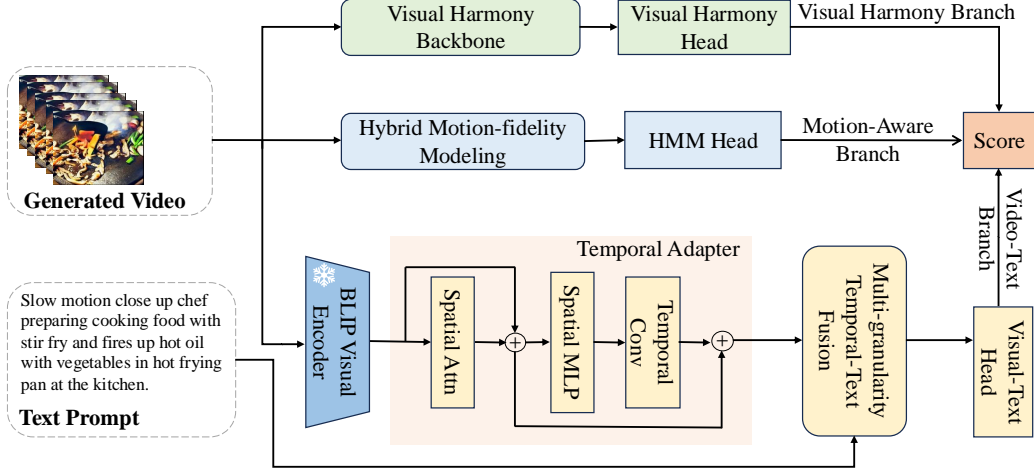


Figure 5. Network overview of the proposed CRAVE.

to scoring, all participants were gathered on-site for training. During the training, we presented some cases outside the dataset, including good, bad, and average examples, to ensure a basic understanding of the task. The scoring was conducted on-site, with a mandatory 5-minute break after every 15 minutes of scoring to prevent fatigue. Based on prior work (Sun et al., 2024b; 2025), the scoring system used a 10-point scale. During the scoring, the annotators were advised to assess the video from three perspectives: (1) visual quality, which is commonly used in traditional VQA methods; (2) matching between the text and video; and (3) motion quality, such as whether motion consistency is maintained, whether the motion is distorted, and whether it aligns with common sense. Following prior works (Kou et al., 2024b; Liu et al., 2024a), to better estimate the total score of the video, the subjects were asked to provide a final overall score after considering all three aspects. After all the scoring was completed, we obtained a total of 35,612 subjective scores, from which we derived the raw MOS score. As shown in Figure 4, we then normalize the raw scores as Z-score MOS, which could be formulated as:

$$MOS_z(m, i) = \frac{X_{m,i} - \mu(X_i)}{\sigma(X_i)}, \quad (1)$$

where $X_{m,i}$ and $MOS_z(m, i)$ denotes the raw and Z-score MOS of m -th video of i -th annotator, respectively. $\mu(\cdot)$ and $\sigma(\cdot)$ refer to the mean and standard deviation function, respectively. X_i represents all MOS from the i -th annotator. After deriving $MOS_z(m, i)$, the screening method in BT.500 (Int.Telecommun.Union, 2000) is deployed to filter the outliers.

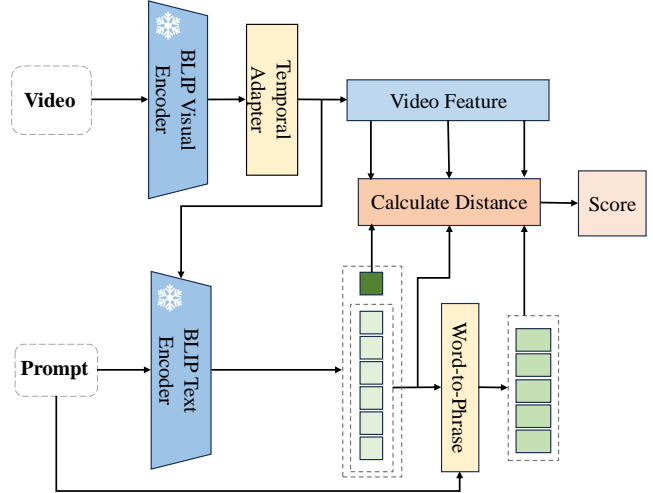


Figure 6. Details of the proposed MTT module for text alignment.

4. Content-Rich AIGC Video Evaluator

4.1. Overall Framework

CRAVE evaluates content-rich AIGC videos from three perspectives: (1) visual harmony, measured using traditional video quality metrics like aesthetics and distortion, (2) text-video semantic alignment, achieved via Multi-granularity Text-Temporal (MTT) fusion, and (3) motion-aware consistency, which is specific for dynamic distortions in AIGC videos, captured through Hybrid Motion-fidelity Modeling (HMM). The overall framework is illustrated in Figure 5. We will delve into the details of each module in the following sections.

4.2. Visual Harmony

For traditional natural video quality assessment, we utilize DOVER (Wu et al., 2023a) to assess individual videos from the aesthetic and technical perspectives given its success. DOVER evaluates videos based on two dimensions: aesthetic score and technical distortion. In this work, we use the pre-trained DOVER method as the Visual Harmony Backbone, followed by a linear head to obtain the output, which could be formulated as:

$$F_{aes} = \Phi_{aes}(V), \quad (2)$$

$$F_{tech} = \Phi_{tech}(V), \quad (3)$$

$$O_{vh} = \omega_{vh}(F_{aes} \oplus F_{tech}), \quad (4)$$

where V is the input video, Φ_{aes} , Φ_{tech} represent the aesthetic encoder and distortion encoder in DOVER, respectively, \oplus denotes concatenation along the dimension, ω_{vh} represents the linear head for this branch, and O_{vh} refers to the corresponding output.

4.3. Multi-Granularity Text-Temporal Fusion

Multi-granularity Text-Temporal (MTT) module firstly leverages high-quality priors from multi-modal understanding approaches like BLIP (Li et al., 2022b), successfully extending it in the temporal dimension via effective temporal adapters. Then the visual information aggregated in the temporal adapter interacts with the text embedding via cross-attention. To flexibly fuse effective information from the text, we additionally perform multi-granularity aggregation on the text. Namely, in addition to the whole input, we break down the text into phrases and words of varying granularity containing different levels of semantic information via SpaCy (Honnibal et al., 2020). After that, the integrated text embeddings of varying granularity are measured with the output of the visual branch, as shown in Figure 6. The entire process can be formulated as:

$$F_v = \Phi_t(\Phi_s(V)), \quad (5)$$

$$F_e = \Phi_e(\text{Concat}([enc], F_v), e), \quad (6)$$

$$F_{enc} = F_e[0, \dots], \quad (7)$$

$$F_{word} = F_e[1 :, \dots], \quad (8)$$

where V , e , F_v are the input video, text prompt, and the derived visual feature, respectively. Φ_s , Φ_t , Φ_e denote the spatial encoder, temporal adapter, and text encoder, respectively. F_{enc} and F_{word} refer to the $[enc]$ token embedding and the word token embedding, representing different levels of semantics of the textual prompt. To get the phrase-level encoding for prompts, we utilize the successful word-to-phrase module in (Zhu et al., 2023). The module converts the mapping between word and phrase to the mapping between word embedding and phrase embedding, based on the position mapping between word and the corresponding

embedding, which could be formulated as,

$$\{p_1, p_2 \dots, p_m\} = \Phi_w(\{w_1, w_2 \dots, w_n\}), \quad (9)$$

$$\{F_{p_1}, F_{p_2} \dots, F_{p_m}\} = \Phi_{F_w}(\{F_{w_1}, F_{w_2} \dots, F_{w_n}\}), \quad (10)$$

where Φ_w and Φ_{F_w} refer to the mapping between word and phrase and the mapping between word embedding and phrase embedding. p_i , w_i refers to the i -th useful phrase and word in prompt, while F_{p_i} , F_{w_i} refers to the i -th phrase embedding and word embedding, respectively.

After that, we calculate the cosine distance between all text features and video features respectively. Finally, we sum them up to get the final score.

$$O_{align} = \sum_l \cos(F_l, F_v), \quad (11)$$

where l denotes different levels of granularity such as the whole paragraph level, phrase level and word level.

4.4. Hybrid Motion-fidelity Modeling

Compared with natural videos, AIGC videos usually contain unique distortions such as irregular objects and motions that violate the physical laws. Despite significant improvements in recent video generation models, low-fidelity motion remains a persistent challenge. Here, motions that defy logic, deformed motions, and motions with abnormal amplitudes are collectively referred to as "low-quality" motions. To better assess motion distortions in current AIGC videos, we propose Hybrid Motion-fidelity Modeling (HMM), which hierarchically captures motion features at different granularities. Specifically, considering the successful application of optical flow in anomaly detection (Caldelli et al., 2021; Agarwal et al., 2020), we leverage dense motion information derived from optical flow to capture low-level motion patterns, combined with global abstract motion information from action recognition tasks (Kay et al., 2017; Goyal et al., 2017). The experimental section later demonstrates the effectiveness of combining these two aspects. In practice, flow features are extracted using the pre-trained StreamFlow (Sun et al., 2024c), while high-level abstract motion priors are obtained from the pre-trained Uniformer (Li et al., 2023). Different branches are then input into the feed-forward network and pass through a linear head to regress and obtain the final output.

4.5. Supervision

Based on the previous training objective in (Wu et al., 2023a; 2022; Sun et al., 2022b), the mix of rank loss (Gao et al., 2019) and PLCC (Pearson Linear Correlation Coefficient) loss are adopted to train the overall network. Note that the BLIP visual and text encoder remains frozen throughout the training process. The whole training objective could be

formulated as,

$$\mathcal{L} = \mathcal{L}_{plcc} + \gamma \cdot \mathcal{L}_{rank}, \quad (12)$$

where γ is the coefficient set to 0.3 in the experiments.

5. Experiments

5.1. Implement Details

We use T2VQA-DB (Kou et al., 2024b) and the proposed CRAVE-DB for evaluation. T2VQA-DB is the largest AIGC VQA dataset for text-driven video generation. It contains plenty of AIGC videos from previous methods, which provides a good complement to the evaluation. When training on T2VQA-DB, we use the 10-fold cross-validation, which randomly partitions the whole dataset into 10 equal-sized folds and uses 9 folds for training and 1 fold for testing. We follow the training settings in DOVER (Wu et al., 2023a) and models are trained for 20 epochs with linear probing and then fine-tuned with full parameters for 10 epochs. For CRAVE-DB, we train 40 epochs on the training split and evaluate on the test set. We use the Adam optimizer with the initial learning rate of $1e - 3$ and batch size of 8.

Table 2. Quantitative comparison on CRAVE-DB.

Type	Models	SRCC	PLCC	KRCC
0-shot	UMTScore (Liu et al., 2023)	0.0134	0.0355	0.0118
	Flicker (Huang et al., 2024b)	0.0761	0.0687	0.0493
	Bg. Consis. (Huang et al., 2024b)	0.1170	0.0829	0.0773
	Sub. Consis. (Huang et al., 2024b)	0.1418	0.0956	0.0936
	ViCLIP (Wang et al., 2023d)	0.1290	0.1207	0.0857
	LongCLIP (Zhang et al., 2024)	0.2757	0.3033	0.1884
	Aes. Score (Huang et al., 2024b)	0.3557	0.3457	0.2373
	HPSv2 (Wu et al., 2023c)	0.0562	0.0501	0.0391
	PickScore (Kirstain et al., 2023)	0.0557	0.0492	0.0361
	ImageReward (Xu et al., 2023)	0.2216	0.2125	0.1470
	Motion Sm. (Huang et al., 2024b)	0.2331	0.2630	0.1549
Ft.	SimpleVQA (Sun et al., 2022b)	0.6230	0.6180	0.4436
	StableVQA (Kou et al., 2023)	0.6396	0.6415	0.4552
	FastVQA (Wu et al., 2022)	0.7155	0.7062	0.5243
	DOVER (Wu et al., 2023a)	0.7095	0.7192	0.5224
	TriVQA (Qu et al., 2024)	0.7183	0.7313	0.5293
T2VQA (Kou et al., 2024b)	0.7266	0.7098	0.5369	
Ours	CRAVE	0.7587	0.7581	0.5660

5.2. Quantitative Results

As shown in Table 3 and Table 2, we can learn that CRAVE achieves leading performance on both the proposed content-rich dataset and the T2VQA-DB, which includes prior AIGC videos. On CRAVE-DB, CRAVE demonstrates a particularly significant lead, highlighting its effectiveness in evaluating next-generation AIGC videos. On T2VQA-DB, CRAVE also outperforms previous models, even surpassing LLM-based models such as Q-Align and T2VQA, which further demonstrates the effectiveness of its multidimensional design. ‘‘Ft.’’ denotes methods that need further fine-tuning

Table 3. Quantitative comparison on T2VQA-DB.

Type	Models	SRCC	PLCC	KRCC
0-shot	CLIPSim (Radford et al., 2021)	0.1047	0.1277	0.0702
	BLIP (Li et al., 2022b)	0.1659	0.1860	0.1112
	ImageReward (Xu et al., 2023)	0.1875	0.2121	0.1266
	ViCLIP (Wang et al., 2023d)	0.1162	0.1449	0.0781
	UMTScore (Liu et al., 2023)	0.0676	0.0721	0.0453
Ft.	SimpleVQA (Sun et al., 2022b)	0.6275	0.6338	0.4466
	BVQA (Li et al., 2022a)	0.7390	0.7486	0.5487
	FastVQA (Wu et al., 2022)	0.7173	0.7295	0.5303
	DOVER (Wu et al., 2023a)	0.7609	0.7693	0.5704
	Q-Align (Wu et al., 2023b)	0.7601	0.7768	0.5860
	T2VQA (Kou et al., 2024b)	0.7965	0.8066	0.6058
Ours	CRAVE	0.8122	0.8214	0.6338

on the target dataset. ‘‘Bg.’’, ‘‘Sub.’’, ‘‘Consis’’, ‘‘Aes.’’, ‘‘Sm.’’ denote the background, subject, consistency, aesthetic, and smoothness, respectively. 0-shot methods tend to have lower results, which is also observed in previous works (Kou et al., 2024b; Sun et al., 2024b). It could be due to the lack of alignment with human perception or the consideration of the dynamic distortion in AIGC videos.

5.3. Qualitative Results

We visualize the difference between the predicted and the ground-truth MOS, as shown in the supplements. The curves are obtained from a fourth-order polynomial nonlinear fitting. We further present the scores of different AIGC videos assessed via CRAVE in the supplements.

5.4. Zero-Shot Ranking Comparison

We present the rankings of next-generation video generation model scores evaluated by CRAVE after training on different VQA datasets. As discussed in Section 3.2, VideoGenEval (Zeng et al., 2024) was selected for this experiment due to its relatively high prompt density, its completely distinct data sources compared to CRAVE-DB, and its inclusion of newer models. We utilized all 424 text-to-video (t2v) prompts and generated results from VideoGenEval, which include recent models such as (Zhipu, 2024; Shengshu, 2024; Team, 2024; Brooks et al., 2024; Yang et al., 2024; LumaLabs, 2024; ByteDance, 2024; Hunyuan, 2024; Runway, 2024; Kuaishou, 2024). As shown in Figure 7, (a) and (b) correspond to CRAVE using the pretrained weights in Table 3 and Table 2, respectively.

5.5. Ablation Study

To verify the effectiveness of the proposed method, we ablate each component on the design of CRAVE, as shown in Table 4. Underlined settings are used in our final model. We conducted experiments on both CRAVE-DB

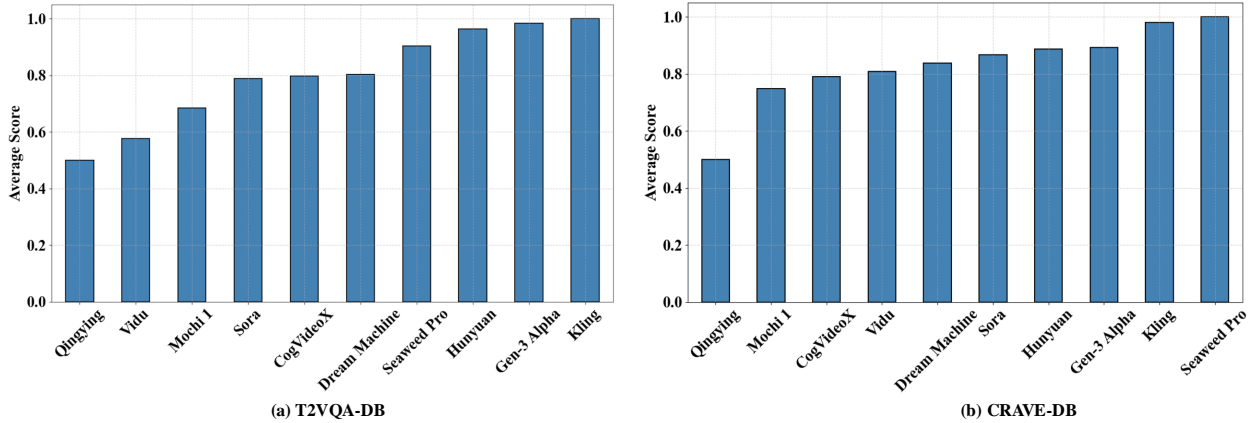


Figure 7. The ranking of next-generation models provided by models trained on different AIGC VQA datasets.

Table 4. Quantitative results of ablation study.

Experiment	Method	CRAVE-DB			T2VQA-DB		
		SRCC	PLCC	KRCC	SRCC	PLCC	KRCC
Temporal-Text Fusion	None	0.6512	0.6601	0.4643	0.7701	0.7804	0.5885
	ST-Graph.	0.6966	0.6968	0.5042	0.7990	0.8084	0.6196
	Temp. Attn.	0.7159	0.7175	0.5226	0.7989	0.8089	0.6199
	<u>Pseudo 3D Conv</u>	0.7310	0.7241	0.5335	0.8077	0.8167	0.6289
Multi-Granularity Text Injection	None	0.7477	0.7458	0.5526	0.8077	0.8167	0.6289
	Global	0.7520	0.7485	0.5566	0.8115	0.8207	0.6329
	Local	0.7524	0.7498	0.5578	0.8121	0.8212	0.6337
	<u>Individual Combined</u>	0.7587	0.7581	0.5660	0.8122	0.8214	0.6338
Motion-Aware Modeling	None	0.7507	0.7499	0.5561	0.8103	0.8199	0.6317
	High-Level	0.7527	0.7529	0.5605	0.8111	0.8204	0.6326
	Low-Level	0.7529	0.7513	0.5576	0.8118	0.8211	0.6330
	<u>Hybrid</u>	0.7587	0.7581	0.5660	0.8122	0.8214	0.6338
Flow Frames	4	0.7562	0.7552	0.5598	0.8110	0.8206	0.6323
	8	0.7566	0.7564	0.5612	0.8113	0.8208	0.6326
	<u>16</u>	0.7587	0.7581	0.5660	0.8122	0.8214	0.6338

and T2VQA-DB. As CRAVE-DB naturally contains intricate texts, rich motion information, and other such content, We could learn that the improvements on CRAVE-DB are generally more significant. We first explore ways to align the text with temporal visual information. ST-Graph, namely the spatiotemporal graph, flattens the time dimension into the spatial dimension for calculation. Temp. Attn. denotes the attention along the additional temporal dimension. Pseudo 3D Conv is inspired by (Singer et al., 2023), where additional convolutions are stacked in the temporal dimension. We can see that the effectiveness has significantly improved with temporal modeling, and that the Pseudo 3D Conv widely used in generation tasks also excels in long-text spatiotemporal modeling. We further investigate the granularity of MTT and discover that integrating all granularity levels yields optimal performance. Additionally, we examine the impact of motion-aware temporal modeling.

Our experiments demonstrate that dense data from optical flow enhances overall performance, and incorporating sparse abstract spatiotemporal information provides a significant performance boost. We further explored the impact of flow frames on the results. Specifically, we calculated the optical flow using 4 frames, 8 frames, and 16 frames during the process. We observed that using more optical flow frames tends to improve accuracy. Given the trade-off between accuracy and efficiency, we ultimately chose 16 frames for the flow calculation.

6. Conclusion

Given the gap between current AIGC videos and AIGC VQA dataset, we introduce CRAVE, an effective VQA method, and CRAVE-DB, a new benchmark for the next-generation AIGC videos. Based on the effective

multi-dimensional design, CRAVE achieves excellent human-aligned results across multiple metrics and datasets. CRAVE-DB contains more content-rich prompts and detailed content, along with extensive human annotations, making it closer to the concurrent text-driven AIGC videos.

Impact Statement

This paper presents work whose goal is to advance the field of Machine Learning. There are many potential societal consequences of our work, none which we feel must be specifically highlighted here.

References

- Achiam, J., Adler, S., Agarwal, S., Ahmad, L., Akkaya, I., Aleman, F. L., Almeida, D., Altenschmidt, J., Altman, S., Anadkat, S., et al. Gpt-4 technical report. *arXiv preprint arXiv:2303.08774*, 2023.
- Agarwal, S., Farid, H., El-Gaaly, T., and Lim, S.-N. Detecting deep-fake videos from appearance and behavior. In *2020 IEEE international workshop on information forensics and security (WIFS)*, pp. 1–6. IEEE, 2020.
- Blattmann, A., Dockhorn, T., Kulal, S., Mendelevitch, D., Kilian, M., Lorenz, D., Levi, Y., English, Z., Voleti, V., Letts, A., et al. Stable video diffusion: Scaling latent video diffusion models to large datasets. *arXiv preprint arXiv:2311.15127*, 2023.
- Brooks, T., Peebles, B., Holmes, C., DePue, W., Guo, Y., Jing, L., Schnurr, D., Taylor, J., Luhman, T., Luhman, E., Ng, C., Wang, R., and Ramesh, A. Video generation models as world simulators. Technical report, OpenAI, 2024.
- ByteDance. Seaweed pro. <https://jimeng.jianying.com/>, 2024.
- Caldelli, R., Galteri, L., Amerini, I., and Del Bimbo, A. Optical flow based cnn for detection of unlearned deepfake manipulations. *Pattern Recognition Letters*, 146:31–37, 2021.
- Chai, W., Guo, X., Wang, G., and Lu, Y. Stablevideo: Text-driven consistency-aware diffusion video editing. In *Proceedings of the IEEE/CVF International Conference on Computer Vision*, pp. 23040–23050, 2023.
- Chen, H., Xia, M., He, Y., Zhang, Y., Cun, X., Yang, S., Xing, J., Liu, Y., Chen, Q., Wang, X., et al. Videocrafter1: Open diffusion models for high-quality video generation. *arXiv preprint arXiv:2310.19512*, 2023a.
- Chen, Z., Wu, J., Wang, W., Su, W., Chen, G., Xing, S., Zhong, M., Zhang, Q., Zhu, X., Lu, L., Li, B., Luo, P., Lu, T., Qiao, Y., and Dai, J. Internvl: Scaling up vision foundation models and aligning for generic visual-linguistic tasks. *arXiv preprint arXiv:2312.14238*, 2023b.
- Chivileva, I., Lynch, P., Ward, T. E., and Smeaton, A. F. Measuring the quality of text-to-video model outputs: Metrics and dataset. *arXiv preprint arXiv:2309.08009*, 2023.
- Gao, F., Tao, D., Gao, X., and Li, X. Learning to rank for blind image quality assessment, 2019.
- Goyal, R., Ebrahimi Kahou, S., Michalski, V., Materzynska, J., Westphal, S., Kim, H., Haenel, V., Fruend, I., Yianilos, P., Mueller-Freitag, M., et al. The” something something” video database for learning and evaluating visual common sense. In *Proceedings of the IEEE international conference on computer vision*, pp. 5842–5850, 2017.
- Ho, J., Jain, A., and Abbeel, P. Denoising diffusion probabilistic models. *Advances in neural information processing systems*, 33:6840–6851, 2020.
- Honnibal, M., Montani, I., Van Landeghem, S., and Boyd, A. spacy: Industrial-strength natural language processing in python. 2020. doi: 10.5281/zenodo.1212303.
- Huang, Z., He, Y., Yu, J., Zhang, F., Si, C., Jiang, Y., Zhang, Y., Wu, T., Jin, Q., Chanpaisit, N., Wang, Y., Chen, X., Wang, L., Lin, D., Qiao, Y., and Liu, Z. Vbench: Comprehensive benchmark suite for video generative models. In *Proceedings of the IEEE/CVF Conference on Computer Vision and Pattern Recognition*, 2024a.
- Huang, Z., He, Y., Yu, J., Zhang, F., Si, C., Jiang, Y., Zhang, Y., Wu, T., Jin, Q., Chanpaisit, N., et al. Vbench: Comprehensive benchmark suite for video generative models. In *Proceedings of the IEEE/CVF Conference on Computer Vision and Pattern Recognition*, pp. 21807–21818, 2024b.
- Hunyuan, T. Hunyuanvideo: A systematic framework for large video generative models, 2024. URL <https://arxiv.org/abs/2412.03603>.
- Int.Telecommun.Union. Methodology for the subjective assessment of the quality of television pictures itu-r recommendation. *Tech. Rep.*, 2000.
- Kay, W., Carreira, J., Simonyan, K., Zhang, B., Hillier, C., Vijayanarasimhan, S., Viola, F., Green, T., Back, T., Natsev, P., et al. The kinetics human action video dataset. *arXiv preprint arXiv:1705.06950*, 2017.
- Kirstain, Y., Polyak, A., Singer, U., Matiana, S., Penna, J., and Levy, O. Pick-a-pic: An open dataset of user preferences for text-to-image generation. *Advances in Neural Information Processing Systems*, 36:36652–36663, 2023.

- Kou, T., Liu, X., Sun, W., Jia, J., Min, X., Zhai, G., and Liu, N. Stablevqa: A deep no-reference quality assessment model for video stability. In *Proceedings of the 31st ACM International Conference on Multimedia*, pp. 1066–1076, 2023.
- Kou, T., Liu, X., Zhang, Z., Li, C., Wu, H., Min, X., Zhai, G., and Liu, N. Subjective-aligned dataset and metric for text-to-video quality assessment, 2024a. URL <https://arxiv.org/abs/2403.11956>.
- Kou, T., Liu, X., Zhang, Z., Li, C., Wu, H., Min, X., Zhai, G., and Liu, N. Subjective-aligned dataset and metric for text-to-video quality assessment. *arXiv preprint arXiv:2403.11956*, 2024b.
- Kuaishou. Kling. <https://kling.kuaishou.com/>, 2024.
- Lab, P.-Y. and etc., T. A. Open-sora-plan, April 2024. URL <https://doi.org/10.5281/zenodo.10948109>.
- Labs, P. Pika 1.5. <https://pika.art>, 2024.
- Li, B., Zhang, W., Tian, M., Zhai, G., and Wang, X. Blindly assess quality of in-the-wild videos via quality-aware pre-training and motion perception. *IEEE Transactions on Circuits and Systems for Video Technology*, 32(9):5944–5958, 2022a.
- Li, J., Li, D., Xiong, C., and Hoi, S. Blip: Bootstrapping language-image pre-training for unified vision-language understanding and generation. In *ICML*, 2022b.
- Li, K., Wang, Y., Zhang, J., Gao, P., Song, G., Liu, Y., Li, H., and Qiao, Y. Uniformer: Unifying convolution and self-attention for visual recognition. *IEEE Transactions on Pattern Analysis and Machine Intelligence*, 45(10):12581–12600, 2023.
- Liu, X., Min, X., Zhai, G., Li, C., Kou, T., Sun, W., Wu, H., Gao, Y., Cao, Y., Zhang, Z., Wu, X., Timofte, R., Peng, F., Fu, H., Ming, A., Wang, C., Ma, H., He, S., Dou, Z., Chen, S., Zhang, H., Xie, H., Wang, C., Chen, B., Zeng, J., Yang, J., Wang, W., Fang, X., Lv, X., Yan, J., Zhi, T., Zhang, Y., Li, Y., Li, Y., Xu, J., Liu, J., Liao, Y., Li, J., Yu, Z., Guan, F., Lu, Y., Li, X., Motamednia, H., Hosseini-Benvidi, S. F., Mahmoudi-Aznavah, A., Mansouri, A., Gankhuyag, G., Yoon, K., Xu, Y., Fan, H., Kong, F., Zhao, S., Dong, W., Yin, H., Zhu, L., Wang, Z., Huang, B., Saha, A., Mishra, S., Gupta, S., Sureddi, R., Saha, O., Celona, L., Bianco, S., Napoletano, P., Schettini, R., Yang, J., Fu, J., Zhang, W., Cao, W., Liu, L., Peng, H., Yuan, W., Li, Z., Cheng, Y., Deng, Y., Li, H., Qu, B., Li, Y., Luo, S., Wang, S., Gao, W., Lu, Z., Conde, M. V., Timofte, R., Wang, X., Chen, Z., Liao, R., Ye, Y., Wang, Q., Li, B., Zhou, Z., Geng, M., Chen, R., Tao, X., Liang, X., Sun, S., Ma, X., Li, J., Yang, M., Xu, H., Zhou, J., Zhu, S., Yu, B., Chen, P., Xu, X., Shen, J., Duan, Z., Asadi, E., Liu, J., Yan, Q., Qu, Y., Zeng, X., Wang, L., and Liao, R. Ntire 2024 quality assessment of ai-generated content challenge. In *Proceedings of the IEEE/CVF Conference on Computer Vision and Pattern Recognition (CVPR) Workshops*, pp. 6337–6362, June 2024a.
- Liu, Y., Li, L., Ren, S., Gao, R., Li, S., Chen, S., Sun, X., and Hou, L. Fetv: A benchmark for fine-grained evaluation of open-domain text-to-video generation. *arXiv preprint arXiv: 2311.01813*, 2023.
- Liu, Y., Cun, X., Liu, X., Wang, X., Zhang, Y., Chen, H., Liu, Y., Zeng, T., Chan, R., and Shan, Y. Evalcrafter: Benchmarking and evaluating large video generation models. In *Proceedings of the IEEE/CVF Conference on Computer Vision and Pattern Recognition*, pp. 22139–22149, 2024b.
- LumaLabs. Dream machine. <https://lumalabs.ai/dream-machine>, 2024.
- MiniMax. Hailuo ai. <https://hailuoai.com/video>, 2024.
- Qu, B., Liang, X., Sun, S., and Gao, W. Exploring aigc video quality: A focus on visual harmony, video-text consistency and domain distribution gap. *arXiv preprint arXiv:2404.13573*, 2024.
- Radford, A., Kim, J. W., Hallacy, C., Ramesh, A., Goh, G., Agarwal, S., Sastry, G., Askell, A., Mishkin, P., Clark, J., et al. Learning transferable visual models from natural language supervision. In *International conference on machine learning*, pp. 8748–8763. PMLR, 2021.
- Rombach, R., Blattmann, A., Lorenz, D., Esser, P., and Ommer, B. High-resolution image synthesis with latent diffusion models. In *Proceedings of the IEEE/CVF conference on computer vision and pattern recognition*, pp. 10684–10695, 2022.
- Runway. Gen-3. <https://runwayml.com/blog/introducing-gen-3-alpha/>, 2024.
- Salimans, T., Goodfellow, I., Zaremba, W., Cheung, V., Radford, A., and Chen, X. Improved techniques for training gans. *Advances in neural information processing systems*, 29, 2016.
- Series, B. Methodology for the subjective assessment of the quality of television pictures. *Recommendation ITU-R BT*, 500(13), 2012.
- Shengshu. Vidu. <https://www.vidu.studio/create>, 2024.

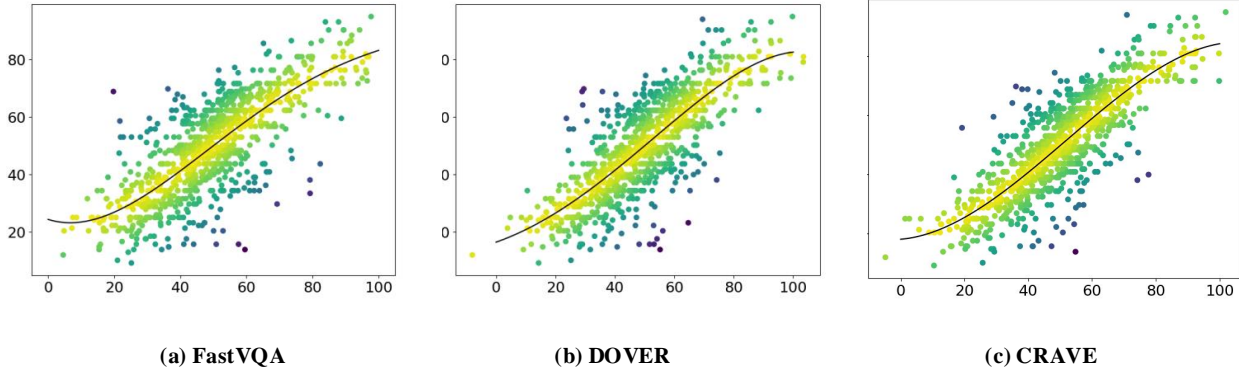
- Singer, U., Polyak, A., Hayes, T., Yin, X., An, J., Zhang, S., Hu, Q., Yang, H., Ashual, O., Gafni, O., et al. Make-a-video: Text-to-video generation without text-video data. In *The Eleventh International Conference on Learning Representations*, 2023.
- Sun, K., Huang, K., Liu, X., Wu, Y., Xu, Z., Li, Z., and Liu, X. T2v-compbench: A comprehensive benchmark for compositional text-to-video generation. *arXiv preprint arXiv:2407.14505*, 2024a.
- Sun, S., Chen, Y., Zhu, Y., Guo, G., and Li, G. Skflow: Learning optical flow with super kernels. *Advances in Neural Information Processing Systems*, 35:11313–11326, 2022a.
- Sun, S., Liang, X., Fan, S., Gao, W., and Gao, W. Ve-bench: Subjective-aligned benchmark suite for text-driven video editing quality assessment. In *Proceedings of the AAAI Conference on Artificial Intelligence*, 2024b.
- Sun, S., Liu, J., Li, T. H., Li, H., Liu, G., and Gao, W. Streamflow: Streamlined multi-frame optical flow estimation for video sequences. In *Advances in neural information processing systems*, 2024c.
- Sun, S., Qu, B., Liang, X., Fan, S., and Gao, W. Ie-bench: Advancing the measurement of text-driven image editing for human perception alignment. *arXiv preprint arXiv:2501.09927*, 2025.
- Sun, W., Min, X., Lu, W., and Zhai, G. A deep learning based no-reference quality assessment model for ugc videos. In *Proceedings of the 30th ACM International Conference on Multimedia*, pp. 856–865, 2022b.
- Team, G. Mochi 1. <https://github.com/genmoai/models>, 2024.
- Teed, Z. and Deng, J. Raft: Recurrent all-pairs field transforms for optical flow. In *Computer Vision—ECCV 2020: 16th European Conference, Glasgow, UK, August 23–28, 2020, Proceedings, Part II 16*, pp. 402–419. Springer, 2020.
- Tongyi, A. Wanxiang video. <https://tongyi.aliyun.com/wanxiang/videoCreation>, 2024.
- Unterthiner, T., Van Steenkiste, S., Kurach, K., Marinier, R., Michalski, M., and Gelly, S. Towards accurate generative models of video: A new metric & challenges. *arXiv preprint arXiv:1812.01717*, 2018.
- Wang, J., Yuan, H., Chen, D., Zhang, Y., Wang, X., and Zhang, S. Modelscope text-to-video technical report. *arXiv preprint arXiv:2308.06571*, 2023a.
- Wang, Y., Chen, X., Ma, X., Zhou, S., Huang, Z., Wang, Y., Yang, C., He, Y., Yu, J., Yang, P., et al. Lavie: High-quality video generation with cascaded latent diffusion models. *arXiv preprint arXiv:2309.15103*, 2023b.
- Wang, Y., Chen, X., Ma, X., Zhou, S., Huang, Z., Wang, Y., Yang, C., He, Y., Yu, J., Yang, P., et al. Lavie: High-quality video generation with cascaded latent diffusion models. *arXiv preprint arXiv:2309.15103*, 2023c.
- Wang, Y., He, Y., Li, Y., Li, K., Yu, J., Ma, X. J., Chen, X., Wang, Y., Luo, P., Liu, Z., Wang, Y., Wang, L., and Qiao, Y. Internvid: A large-scale video-text dataset for multimodal understanding and generation. *ArXiv*, abs/2307.06942, 2023d. URL <https://api.semanticscholar.org/CorpusID:259847783>.
- Wu, H., Chen, C., Hou, J., Liao, L., Wang, A., Sun, W., Yan, Q., and Lin, W. Fast-vqa: Efficient end-to-end video quality assessment with fragment sampling. In *European conference on computer vision*, pp. 538–554. Springer, 2022.
- Wu, H., Zhang, E., Liao, L., Chen, C., Hou, J., Wang, A., Sun, W., Yan, Q., and Lin, W. Exploring video quality assessment on user generated contents from aesthetic and technical perspectives. In *Proceedings of the IEEE/CVF International Conference on Computer Vision*, pp. 20144–20154, 2023a.
- Wu, H., Zhang, Z., Zhang, W., Chen, C., Li, C., Liao, L., Wang, A., Zhang, E., Sun, W., Yan, Q., Min, X., Zhai, G., and Lin, W. Q-align: Teaching Imms for visual scoring via discrete text-defined levels. *arXiv preprint arXiv:2312.17090*, 2023b.
- Wu, X., Hao, Y., Sun, K., Chen, Y., Zhu, F., Zhao, R., and Li, H. Human preference score v2: A solid benchmark for evaluating human preferences of text-to-image synthesis. *arXiv preprint arXiv:2306.09341*, 2023c.
- Xu, J., Liu, X., Wu, Y., Tong, Y., Li, Q., Ding, M., Tang, J., and Dong, Y. Imagereward: Learning and evaluating human preferences for text-to-image generation, 2023.
- Yang, Z., Teng, J., Zheng, W., Ding, M., Huang, S., Xu, J., Yang, Y., Hong, W., Zhang, X., Feng, G., et al. Cogvideox: Text-to-video diffusion models with an expert transformer. *arXiv preprint arXiv:2408.06072*, 2024.
- Zeng, A., Yang, Y., Chen, W., and Liu, W. The dawn of video generation: Preliminary explorations with sora-like models. *arXiv preprint arXiv:2410.05227*, 2024.
- Zhang, B., Zhang, P., Dong, X., Zang, Y., and Wang, J. Long-clip: Unlocking the long-text capability of clip. *arXiv preprint arXiv:2403.15378*, 2024.

Zheng, Z., Peng, X., Yang, T., Shen, C., Li, S., Liu, H., Zhou, Y., Li, T., and You, Y. Open-sora: Democratizing efficient video production for all, March 2024. URL <https://github.com/hpcaitech/Open-Sora>.

Zhipu. Ying. <https://chatglm.cn/video>, 2024.

Zhu, C., Jia, Q., Chen, W., Guo, Y., and Liu, Y. Deep learning for video-text retrieval: a review. *International Journal of Multimedia Information Retrieval*, 12(1):3, 2023.

A. Qualitative Results.



(d) Scores on different videos

Figure 8. Scatter plots of the predicted scores and ground-truth MOSs. A brighter scatter point represents higher density.

As shown in Figure 8, (a), (b), and (c) represent the visualization of the differences between different models on T2VQA-DB. The more clustered the points, the smaller the differences. We can observe that the points in (a) and (b) are more scattered and farther from the central line. A fourth-order polynomial nonlinear fitting is used to draw the central line. (d) shows the scores of CRAVE for the generated results of different models. More detailed videos can be found in the supplementary materials. Here, the direct output of CRAVE has not been normalized, so negative values may occur.